Synergic effect of naphthylated carbon nanotubes and gold nanoparticles on catalytic performance of hybrid films containing bilirubin oxidase for the dioxygen reduction.

Valentina Grippo,[a] Joanna Pawłowska,[a] Jan F. Biernat,[b] Renata Bilewicz [a]

[a] University of Warsaw, Faculty of Chemistry, Pasteura 1, 02-093 Warsaw, Poland

[b] Gdansk University of Technology, Faculty of Chemistry, Narutowicza 11/12, 80-233 Gdansk, Poland

Abstract:

To improve the direct electron transfer from a multicopper oxidase *Mv*BOd to the glassy carbon electrode surface the naphthylated multiwall carbon nanotubes (Napth-MWCNTs) are combined with gold nanoparticles (AuNPs) to form a conductive network at the electrode and increasing its working surface. Such approach allowed to eliminate the necessity of employing mediators to reach elevated current values. The enzyme stability was improved by accommodating it in a biomimetic film of lipidic liquid-crystalline mesophase of cubic symmetry. The cubic phase hosted the enzyme in its fully active form for weeks of continuous work of the electrode.

Keywords: bilirubin oxidase, cubic phase, gold nanoparticles, multi-walled carbon nanotubes, oxygen reduction reaction.

1. Introduction

The oxygen reduction reaction (ORR) is one of the most important chemical processes in living organisms or energy converting systems.[1]

Many studies have been conducted on the multicopper oxidases with the aim of gaining more insight into the ORR mechanism and to reproduce this reaction with higher efficiency.[2]

Bilirubin oxidase (*Mv*BOd) has been found to be the best catalyst for oxygen reduction due to very low overpotential necessary to catalyse the reduction of oxygen to water, and also to the ability to work in solutions containing high concentrations of sodium chloride. [3] *Mv*BOd oxidises bilirubin to biliverdin while the oxygen is reduced to water by electron transfer via the T1 centre and the trinuclear T2/T3 cluster.[4]

Direct electron transfer (DET)-type bioelectrocatalysis has attracted increasing attention in the past decades due to its advantages such as simplified construction of the electrodes, the absence of energy loss caused by participation of mediators, and the absence of problems connected with stability or leaching of mediators from the film to the solution.[5,6]

Unfortunately, most of the enzymes cannot directly communicate with electrodes, because the active centre of enzyme is often embedded deeply in the polypeptide environment. Novel materials and methods have been developed improving the DET-type bioelectrocatalysis. Good performance of DET-type reaction can be achieved by using nano-materials, such as carbon nanotubes [6, 7], Fe_3O_4 magnetic nanoparticle [8], and Au nanoparticles [9], thanks to increased specific surface areas and high conductivity. Direct electron transfer between the enzyme and the electrode can be established via multi-walled carbon nanotubes (MWCNT).[5] A *Mv*BOd MWCNT-Au electrode with covalently bound *Mv*BOd can achieve current densities of 500 $\mu A/cm^2$.[10]

The main goal of our work was to construct an efficient biocathode for the reduction of dioxygen to water based on direct electron transfer in the *Mv*BOd –gold nanoparticles– carbon nanotube conjugate network. Such approach eliminates the use of mediators together with increasing the number of *Mv*BOd molecules in favourable orientation for electron exchange with the electrode. Important for the biofuel cell application: high catalytic current and good stability of the biocathode, can be achieved. Surface modification with naphthylated carbon nanotubes on which *Mv*BOd molecule can be anchored improves both stability and catalytic activity and enables the incorporation of gold nanoparticles. [11]

The stability of the modified surface was improved by the use of a membrane-mimetic matrix that resembles the natural environment: the liquid-crystalline lipidic cubic phase (LCP). Entrapment in cubic phase protects the enzyme from chemical and physical degradation thereby facilitating retention of its native bioactivity. Furthermore, lipids forming the LCPs are non-toxic, biocompatible and biodegradable. [12] Advantages of enzymes hosted in cubic phase have been reported during the past years. When laccase was hosted in the cubic phase mediatorless reduction of oxygen was seen using boron-doped diamond (BDD) as the electrode substrate contrary to using GCE as the electrode. [13] More recently, direct electron transfer between D-Fructose dehydrogenase entrapped in cubic phase and a glassy carbon electrode surface was studied to build a biosensing device for fructose.[14]

2. Materials and methods

2.1. Chemicals

Bilirubin Oxidase from *Myrothecium verrucaria* (25 U·mg^{-1}), and monoolein (1-oleoyl-rac-glycerol) (MO) purchased from Sigma were used as received. Na_2HPO_4, KH_2PO_4, NaCl and KCl were from POCh (Polish Chemicals Co.). All solutions were prepared using MilliQ water (18.2 MΩ·cm^{-1}), from Millipore, Bedford, MA, USA.

2.2. Synthesis of gold nanoparticles

Gold NPs were prepared using a slightly modified Brust-Schiffrin method. An aqueous solution of hydrogen tetrachloroaurate (III) (30 mL, 30 mM) was extracted with 80 mL of tetraoctylammonium bromide (2.19 g, 5 mmol) solution in toluene. Most of the tetrachloroaurate ions were transferred to the organic layer as the yellow aqueous layer faded until colorless. Then, 1.44 µL ($8.3 \cdot 10^{-6}$ M) of 1-octanethiol was added to the organic phase, and the mixture was reduced using a freshly prepared aqueous solution of sodium borohydride (378 mg, 200 mmol in 25 mL of deionized water). A solution of borohydride was very slowly added under vigorous stirring. After further stirring for 3 h, the organic phase was separated, evaporated to 10 mL in a rotary evaporator, and mixed with 400 mL of absolute ethanol to precipitate the NPs. The mixture was kept for 12 h at -4°C. The dark brown precipitate was sonicated for 60 s and centrifuged (5 min, 13 000 rpm). Again, the precipitate was dissolved in a small amount of toluene (10 mL), precipitated with ethanol (400 mL) and centrifuged four times. Finally, all samples were dissolved in 10 mL of toluene. The final concentration is estimated to be 5 mg/mL. The obtained nanoparticles were characterized by TEM and DLS.

2.3. TEM measurements

The morphology and size of obtained gold nanoparticles were determined using a Libra TEM (Carl Zeiss) operating at 120 kV. One or two droplets of as-prepared nanoparticle solutions diluted with toluene to a very low concentration were placed on a standard copper grid (400-mesh) coated with carbon. The grid was left overnight to dry. TEM images of the synthesized AuNPs are shown in Figure 1. The dispersed nanoparticles have an average diameter of 4.75 nm.

2.4. Dynamic Light Scattering

The dynamic light scattering measurements were performed using ZetasizerNano ZS from Malvern Instruments. The size of the octanethiol@AuNPs from the DLS measurements is 5.29 nm, which is in excellent agreement with the TEM results (4.75 nm of the gold core).

2.5. Napht-MWCNTs modification procedure

The modification was carried as reported earlier [15]. After 15 min of sonification of a mixture of pristine MWCNTs (CheapTubes, 40mg), 2-naphthylamine hydrochloride (936 mg), pyridine (0.45 mL), o-dichlorobenzene (5 mL) and acetonitrile (5 mL), the amyl nitrite (0.72 mL) was added. The mixture has been further sonicated at 65°C for 6 h. The solid was then collected by centrifugation, washed in sequence with DMF, methanol, chloroform untilthe washings became colorless. Each washing was accompanied by sonication. Finally the product was dried in vacuum. The product contains not only naphthyl residues bonded to nanotubes, but also naphthylated naphthyl residues. The number of naphthyl residues directly or indirectly bonded to nanotube's carbon atoms equals 0.0061. (synthetic scheme in Supporting Information, S1).

2.6. Voltammetry

Cyclic voltammetry experiments were done using the Autolab potentiostat (ECO Chemie, Netherlands) in a three electrode arrangement, with a silver/silver chloride (Ag/AgCl) electrode as the reference, platinum foil as the counter and the glassy carbon electrode (GCE, BAS, 3 mm diameter) as the working electrode. All experiments were carried out at 25°C. The GC electrode was polished mechanically with 1.0, 0.3 and 0.05 µm alumina powder on a Buehler polishing cloth to a mirror-like surface. Finally, it was rinsed thoroughly with water and sonificated in pure ethanol. All current densities were calculated using the geometrical area of the GCE (A=0.071 cm^2).

2.7. Preparation of the cubic phase

The cubic phases were prepared by melting monoolein in a small glass vial (about 100 mg) and an appropriate amount of phosphate buffer or enzyme solution was added and gold nanoparticles. The ratio of the components was chosen on the basis of the phase diagram for the monoolein–water system and it corresponds to a diamond type of cubic phase.[16] The glass vial was tightly sealed and left for at least 24 h at room temperature for the contents to equilibrate. A transparent and highly viscous cubic phase was obtained. The stability of the system was confirmed by macroscopic observations of the sample viscosity and clarity and by SAXS measurements. The prepared cubic phase was weighed to determine the amount of enzyme in the system. The ''empty'' cubic phase can be stored in a closed vial for several months.[17,18]

2.8. SAXS

Phase identity and structural parameters of the lipidic samples were determined by X-ray diffraction using a Bruker AXS Micro, with a microfocused X-Ray source. The Cu Kα radiation (λCu Kα =1.5418 Å) was collimated by a 2D Kratky-collimator and the data were collected by a 2D Pilatus 100K detector. The scattering vector, q=(4π/λ)sinθ, with 2θ being the scattering angle, was calibrated using silver behenate. Data were collected and azimuthally averaged using the Saxsgui software to yield one-dimensional intensity versus scattering vector q, with q ranging from 0.004 to 0.5 Å^{-1}. Dispersion samples were filled into 2 mm diameter quartz

capillaries sealed with epoxy glue (UHU). Measurements were performed at 25°C and 40°C; scattered intensity was collected over 5 hours. The radius of water channel was determined as described in Supporting information, S2.

3. Results and discussion

3.1. Hybrid film preparation

Four different approaches were studied: A suspension of pure (**a**) or naphthalene functionalized, (**b**) MWCNTs in ethanol (140 μL containing 93 μg of MWCNTs) was dropped onto the glassy carbon electrode surface and left to dry. For biomodification, 10 μL (containing 0.1 mg) *Mv*BOd were added onto the electrode surface in both cases. Third approach (**c**) was a layer by layer (LBL) method, when Napht-MWCNTs (140 μL containing 93 μg of MWCNTs) and AuNPs (20 μL, 0.1 mg) (Fig. 1) were casted on the GCE surface and left to dry. The last layer on the surface was obtained by depositing 20 μL (containing 0.2 mg) *Mv*BOd. For the investigation the stability of the *Mv*BOd bioelectrocatalytic activity one more approach was used (**d**). Electrode surface was modified with 93 μg of Napht-MWCNTs ethanol solution and cubic phase containing *Mv*BOd (ca. 0.2 mg) and AuNPs (0.1 mg). The most advantageous approach was selected based on the limiting current of catalysed dioxygen reduction and durability of electrode.
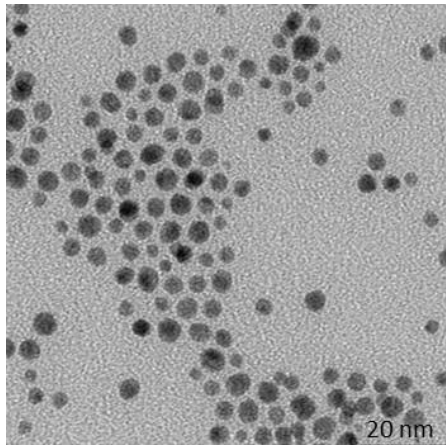

Fig. 1 TEM images of octanethiol@AuNPs

3.2. Electrochemistry of *Mv*BOd adsorbed on glassy carbon electrode covered with Napht-MWCNTs.

*Mv*BOd complete X-ray structure has been solved with a 2.4 Å resolution.[19] It is a blue multicopper oxidase with four redox active Cu atoms. The Cu atoms are assigned type 1 (T1), type 2 (T2) and type 3 (T3) according to their spectroscopic signatures. T2 and T3 form a trinuclear cluster and they are responsible of the water formation. T1 is the one which

MOST WIEDZY Downloaded from mostwiedzy.pl

accepts electrons from the substrate, or from the electrodes and gives those to the trinuclar centre through a Cys-2His electron transfer.[20] The midpoint potential of the T1 site is close to 670 mV vs. NHE while the T2/T3 copper sites are approximately around 400 mV vs. NHE.[21]

In Fig. 2, the cyclic voltammogram is shown for *Mv*BOd modified glassy carbon electrode. The electrode was first covered with 10 µl sample containing 7 µg of naphthylated MWCNTs in PBS buffer. In the voltammogram two redox peaks can be resolved corresponding to the enzyme active sites. The peak corresponding to the reduction of the T2/T3 sites appears at ca. 160 mV *vs.* Ag/AgCl KCl sat. (400mV *vs.* NHE) while the peak for the T1 site appears at ca. 430 mV *vs.* Ag/AgCl KCl sat. (670 mV *vs.* NHE). Therefore, the signal observed corresponds to the reduction of BOd according to the direct electron transfer mechanism as reported by Christenson et al. [21]
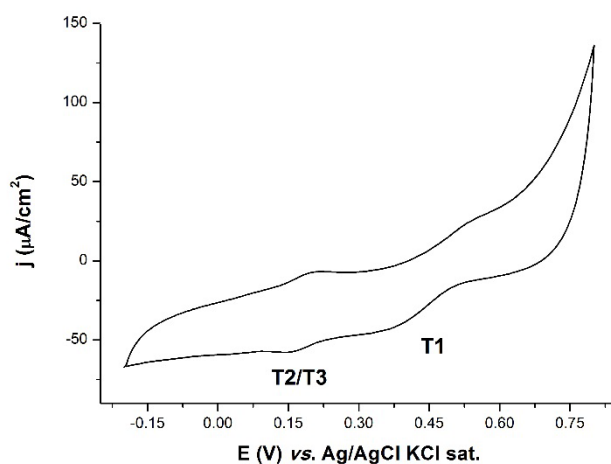

Fig. 2 Cyclic voltammogram of MvBOd modified glassy carbon electrode in the presence of 7 µg of Napth-MWCNTs in PBS buffer solution, pH 7; scan rate: 50 mVs^{-1}.

3.2. Electrocatalytic dioxygen reduction

Electrodes modified with MWCNTs or Napht-MWCNTs conjugates with *Mv*BOd, with or without gold nanoparticles, were used for dioxygen reduction. Those electrodes were characterized by CV under aerobic and anaerobic (Ar purged) conditions. On the glassy carbon electrode covered with MWCNTs and Napth-MWCNTs in the presence of dioxygen, the bioelectrocatalytic oxygen reduction current at pH 7 in PBS and a scan rate of 1 mVs^{-1} was observed. Dioxygen reduction starts at ca. 500 mV vs. Ag/AgCl KCL sat. which is close to the potential of T2 site of *Mv*BOd (Fig. 3). Since no mediators have been added this indicates the DET mechanism is operative and electrons are transferred from the electrode via CNTs to the enzyme and from there to oxygen. Naphthylation of CNTs increased the catalytic current.
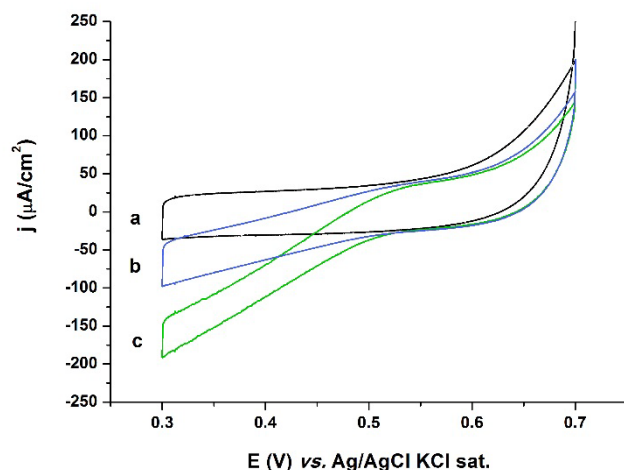
Fig. 3 Comparison of catalytic currents obtained in deoxygenated (**a** - black line) and oxygenated PBS buffer solution, pH 7 recorded with GCE modified with 93 μg of MWCNTs (**b** - blue line) and 93 μg Napht-MWCNTs (**c** - green line) in the presence of 0.1 mg of *Mv*BOd.

The optimal amount of *Mv*BOd was selected for the electrode surface modified with 140 μL (93 μg) of Napth-MWCNTs by increasing the amount of Bilirubin oxidase from 0.033 to 0.5 mg (Fig. 4A). For higher than 0.15mg amounts of *Mv*BOd the limiting current density of the catalytic dioxygen reduction is achieved. Further increase of enzyme amount at the electrode only slightly increased the slope of the waves.
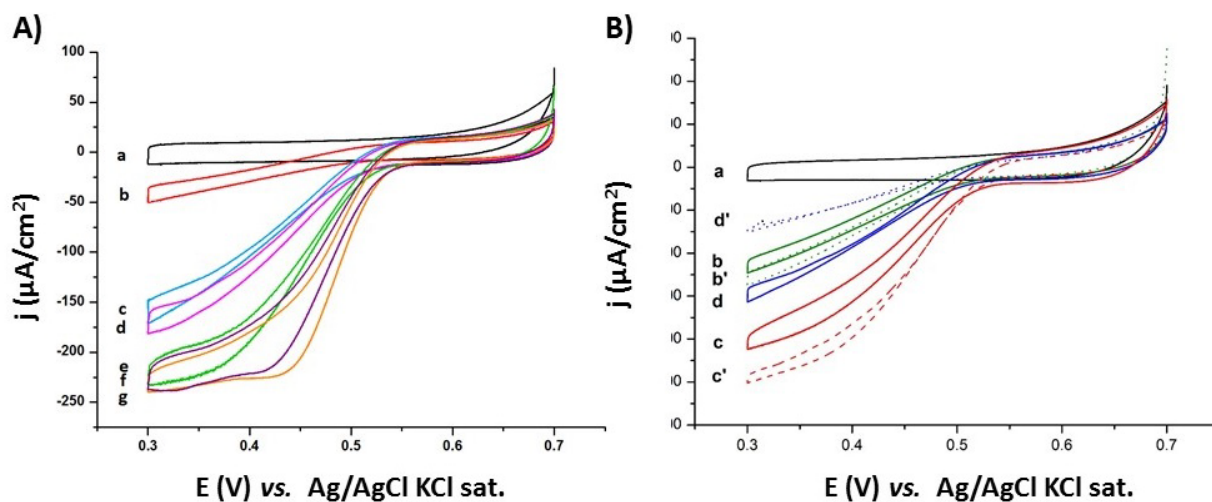

Fig. 4 Cyclic voltammograms recorded for *Mv*BOd catalyzed dioxygen reduction in PBS buffer pH 7, scan rate: 1 mVs^{-1}
(**A**) varying amounts of *Mv*BOd on glassy carbon electrode modified with 93 μg of Napht-MWCNTs: **b**) 0.033 mg; **c**) 0.067 mg; **d**) 0.1 mg; **e**) 0.15 mg; **f**) 0.2 mg; **g**) 0.5 mg.
(**B**) 0.1 mg *Mv*BOd and varying amounts of AuNPs on glassy carbon electrode modified with 93 μg Napht-MWCNTs. Amount of AuNPs: **b**, **b'**: 0.05 mg, **c**, **c'**: 0.1 mg and **d**, **d'**: 0.25 mg in

7

PBS buffer pH 7, scan rate of 1 mVs[-1]. (**b-d**) are for AuNPs placed on top of the nanotube film, dashed lines (**b'-d'**) are for AuNPs placed in between the Napht-MWCNTs layers.
a) as c but in argon saturated solution.

Next step was to optimize the amount of AuNPs using the LBL approach (approach **c**) and the results are shown in Fig. *4*B. Different amounts of AuNPs were placed either on top of the whole Napht-MWCNTs film (4B – b-d) or in between the nanotube layers (4B- b'-d'). The latter forms a composite network on the electrode. The highest value of the catalytic current was observed for GCE modified with 93 µg of Napth-MWCNTs and 0.1 mg of AuNPs. Higher that 0.25mg amounts of AuNPs led to a decrease of the limiting currents and the slope of the wave was smaller probably due to some blocking effects caused by the octanethiol substituents covering the NPs.

In the Supporting Information Fig. S3 we present all the electrode modifications studied. Naphthyl substituted MWCNTs gave always larger catalytic current densities than unmodified MWCNTs. We reported similar observations earlier for dioxygen reduction catalysed by laccase *Cerrena unicolor*. [15] The combination of Napht-MWCNTs and AuNPs in a network was best for adsorbing the enzyme and resulted in the increased value of the biocatalytic dioxygen reduction current.

Largest catalytic current was obtained by combining all the information obtained in the previous stages of research – optimum amount of *Mv*BOd (0.2 mg), 93 µg of Napht-MWCNTs and 0.1 mg of gold nanoparticles deposited on GC electrode covered by the LBL procedure. Fig. *5* shows the catalytic wave with the value of dioxygen reduction current of 650 µA/cm^2. The limiting current of such electrode decreased by ca. 100 µA/cm^2 after each day of work. In order to improve the stability of the catalytic film at longer time scale, the Napth-MWCNTs layer was covered with a layer of lipidic liquid crystalline mesophase of cubic structure containing 0.2 mg BOd and 0.1 mg of AuNPs.
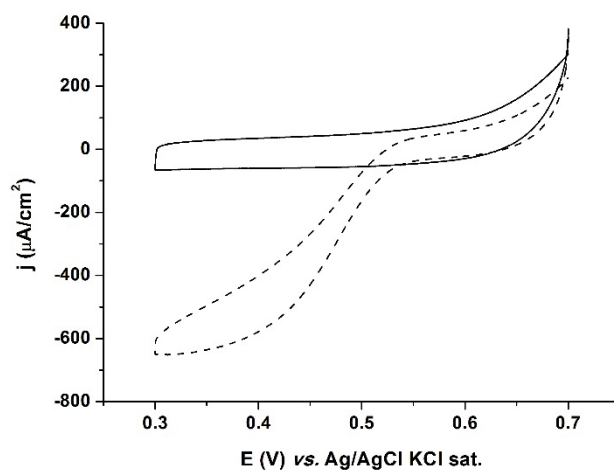
Fig. 5 Cyclic voltammograms recorded in deoxygenated (solid line) and oxygenated (dashed line) PBS buffer solution, pH 7 using 0.2 mg *Mv*BOd on glassy carbon electrode modified with 93 µg Napht-MWCNTs and 0.1 mg of AuNPs, scan rate: 1 mVs^{-1}.

3.3. SAXS measurement of the monoolein cubic phases doped with AuNPs

The X-ray diffraction measurement were done to identify the structure of liquid crystalline phase after doping wit enzyme and NPs. Data were collected for samples prepared in PBS buffer without and with enzyme (Fig. 6A and Fig. 6B). According to the literature, phosphate buffer does not influence the structure of the mesophase. [22] SAXS data for "empty" cubic phase consisting of 60% monoolein prepared at room temperature showed the Pn3m symmetry (Fig. 6A). When 0.04 mg of enzyme was added the same symmetry remained (Fig. 6B). The enzyme is mainly located in cubic phase aqueous channels and does not affect the shape of lipidic bilayer.
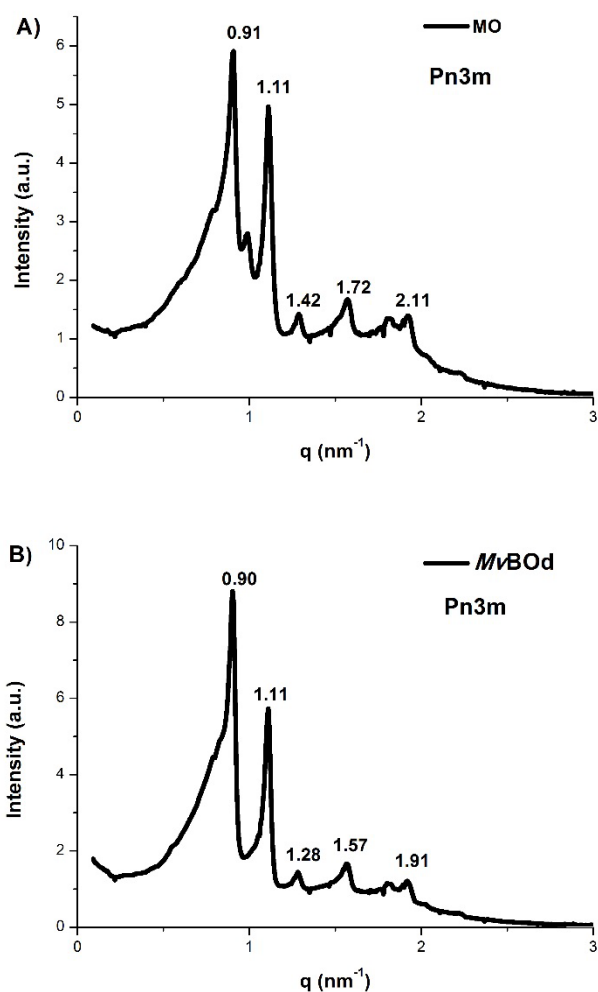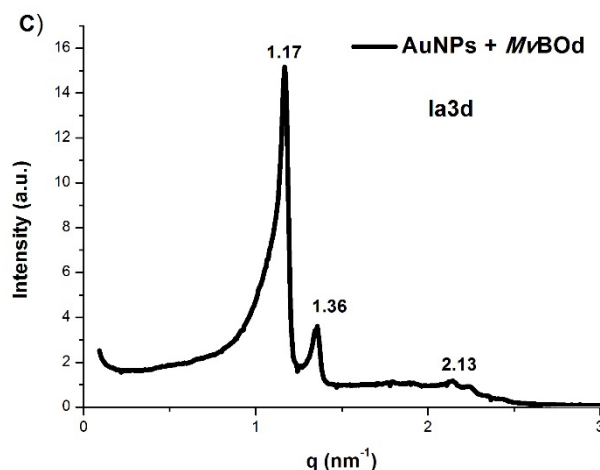
Fig. 6 A) SAXS profile at 25°C of the Pn3m cubic phase containing 60% of MO and 40% of buffer; a: 9.76; d: 4.30 nm. B) SAXS profile at 25°C of the Pn3m cubic phase containing 60% of MO and 40% of *Mv*BOd in buffer; a: 9.87; d: 4.36 nm. C) SAXS profile at 25°C of the Ia3d cubic phase containing 60% of MO-AuNPs and 40% of *Mv*BOd in buffer; a: 13.14; d: 7.50 nm.

Upon incorporation of AuNPs covered with octanethiol molecules (of 4.75 nm diameter) the LCP has still cubic phase symmetry but phase transition from cubic Pn3m to the cubic gyroid phase, Ia3d structure is observed. Most probably the hydrophobic AuNPs are located in part in the lipidic phase and in part in the aqueous channels affecting the water channel width (Table 1).

The lattice parameters do not significantly change their size when temperature is changed from 25°C to 40°C (Supporting Information, S2).

Table Symmetry, lattice parameters, lipid length and aqueous channel diameters for the three monoolein based mesophases *at 25°C*:

Mesophases	Phase symmetry	Lattice parameters a	Lipid length l (nm)	Channel width d (nm)
MO	Pn3m	9.76	1.67	4.30
MO + *Mv*BOd	Pn3m	9.87	1.68	4.36
MO + *Mv*BOd + AuNPs	Ia3d	13.14	1.39	7.50

*calculated according to equations in Supporting Information, S2.

3.4. Effects of cubic phase on the bioelectrocatalytic activity of *Mv*BOd.

The stability of the MvBOd bioelectrocatalytic activity was investigated by measuring the time dependence of the catalytic current of MvBOd adsorbed directly on Napht-MWCNTs /AuNPs/GCE and for the electrode covered with MvBOd in LCP/AuNPs/ Napht-MWCNTs /GCE. In the former case the current density decreased by 40% after only 5 days. The experiments were repeated after storage at 4 °C and at room temperature. The catalytic activity remained more than 70 % of the initial value after 9 days of work of the electrodes covered with Napth-MWCNTs/NPs and BOd in the cubic phase. (Fig. 7) This implies that the GC surface modified with Napht-MWCNTs covered with AuNPs and MvBOd entrapped into the lipidic cubic phase. Therefore, cubic phase entrapment of the enzyme does not improve its catalytic activity towards dioxygen reduction but makes the whole system much more stable on the longer time-scales.
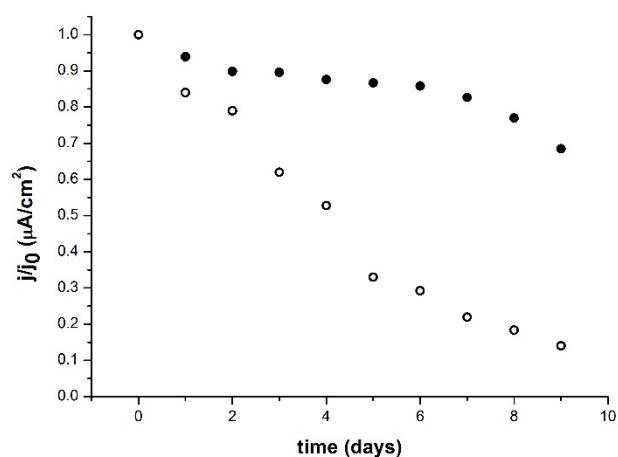

Fig. 7 The long-term stability of MvBOd adsorbed on Napht-MWCNTs /AuNPs/GCE (empty circles) and (MvBOd+ AuNPs) in LCP film on GCE covered with Napht-MWCNTs. (full circles). The activity of the electrode in time is shown as the limiting catalytic current measured at 0.3 V in oxygen-saturated phosphate buffer (pH 7).

Conclusions

The catalysis at the MvBOd modified electrode was improved due to the synergic effect of Napht-MWCNTs forming a network with octanethiol modified gold nanoparticles. The current density was 650 $\mu A/cm^2$ high value as for the direct electron transfer mechanism. Such a high current value makes the system suitable as a biocathode for the biofuel cell. To make the electrode more stable on a longer time-scale the cubic phase film was used to host MvBOd and AuNPs. The stability of the system was increased by the use of the enzyme friendly matrix which is important in the biofuel applications. The current density for the cubic phase film covered electrode was lower than in case of enzyme simply adsorbed on

the AuNPs/Napht-MWCNTs network, however, 70% of the dioxygen reduction current was retained after ten days of work.

Acknowledgments

References:

1. A. A. Gewirth, M.S. Thorum, *Inorg. Chem.*, **2010**, *49*, 3557.
2. E.I. Solomon, J.W. Ginsbach, D.E. Heppner, et al., *Faraday Discuss.*, **2011**, *148*, 11.
3. N. Mano, J. L. Fernandez, Y. Kim, et al., *J. Am. Chem. Soc.,* **2003**, *125*, 15290.
4. Y. Kamitaka, S. Tsujimura, K. Kataoka, et al., *J. Electroanal. Chem.,* **2007**, *601*, 119
5. M.C. Weigel, E. Tritscher, E., F. Lisdat, *Electrochem. Commun.*, **2007**, *9*, 689.
6. M. Zhao, Y. Gao, J. Sun, and F. Gao, *Anal. Chem.*, **2015**, *87*, 2615.
7. G. Sanzó, C. Tortolini, R. Antiochia, et al., *J. Nanosci. Nanotechnol.*, **2015**, *15*, 3423.
8. T. Gu, J. Wang, H. Xia, et al., *Materials*, **2014**, *7*, 1069.
9. V. Krikstolaityte, A. Barrantes, A. Ramanavicius, et al., *Bioelectrochemistry*, **2014**, *95*, 1.
10. K. Schubert, G. Goebel, F. Lisdat, *Electrochimica Acta*, **2009**, *54*, 3033.
11. K. Stolarczyk, D. Łyp, K. Żelechowska, et al., *Electrochimica Acta*, **2012**, *79*, 74.
12. C.V. Kulkarni, W. Wachter, G. Iglesias-Salto, et al., *Phys Chem Chem Phys*, **2011**, *13*, 3004.
13. K. Stolarczyk, E. Nazaruk, J. Rogalski, R. and Bilewicz, *Electrochem. Commun.*, **2007**, *9*, 115.
14. E. Nazaruk, E.M. Landau, R. Bilewicz, *Electrochimica Acta*, **2014**, *140*, 96.
15. D. Majdecka, S. Draminska, K. Stolarczyk, et al., *J. Electrochem. Soc.*, **2015**, *162,* F555.
16. V. Razumas, J. Kanapienené, T. Nylander, et al., 1994, *Anal. Chim. Acta*, **1994**, *289*, 155.
17. P. Rowiński, A. Korytkowska, R. Bilewicz, *Chem. Phys. Lipids*, **2003**, *124*, 147.
18. G. Rummel, A. Hardmeyer, C. Widmer, et al., *J. Struct. Biol.*, **1998**, *121*, 82.
19. J.A. Cracknell, T.P. McNamara, E.D. Lowe, a C.F. Blanford, *Dalton Trans.*, **2011**, *40*, 6668.
20. V. Coman, R. Ludwig, W. Harreither, W., et al., *Fuel Cells*, **2010**, *10*, 9.
21. A. Christenson, S. Shleev, N. Mano, et al., *Biochim. Biophys. Acta BBA - Bioenerg.*, **2006**, *1757*, 1634.
22. E. Nazaruk, E. Górecka, R. Bilewicz, *J. Colloid Interface Sci.*, **2012**, *385*, 130.